Journal of
Ceramic Science
and Technology

J. Ceram. Sci. Tech., **06** [04] 301-304 (2015)
DOI: 10.4416/JCST2015-00042
available online at: http://www.ceramic-science.com

Design, Fabrication and Characterization of Heat Spreaders in Low-Temperature Co-Fired Ceramic (LTCC) utilizing Thick Silver Tape in the Co-Fire Process

T. Welker*, S. Günschmann, N. Gutzeit, J. Müller

Electronics Technology Group, Technische Universität Ilmenau,
Gustav-Kirchhoff-Str. 7, 98693 Ilmenau, Germany

received August 6, 2015; received in revised form September 4, 2015; accepted September 10, 2015

Abstract

Heat spreading in LTCC is commonly realized by means of screen-printed thick film metallization. However, the cross-sectional area of the spreading structure is technologically limited. In the presented investigation, a thick silver tape is used to form a thick silver heat spreader through the LTCC substrate. An opening is structured by laser cutting in the LTCC tape and filled with a laser-cut silver tape. After lamination, the substrate is fired in a constraint sintering process. The bond strength of the silver to LTCC interface is approx. 5.6 MPa. The thermal resistance of the silver structure is measured by means of a thermal test chip glued with a high-thermal-conducting epoxy to the silver structure. The chip contains a resistor and diodes to generate heat and to determine the junction temperature respectively. The rear side of the test structure is temperature-stabilized by means of a temperature-controlled heat sink. The resulting thermal resistance is in the range of 1.1 K/W to 1.5 K/W depending on the length of silver structure (5 mm to 7 mm). Advantages of the presented heat spreader are the low thermal resistance and the good embedding capability in the co-fire LTCC process.

Keywords: LTCC, thermal management, thick silver tape, heat spreader

I. Introduction

Low-Temperature Co-Fired Ceramics (LTCC) are commonly used as substrates for RF (radio frequency) applications owing to the high conductivity and pattern resolution of the conductors and the low loss of the dielectric layer [1–4]. Additionally, the LTCC technology is capturing new markets in the field of fluid- and bioanalytics thanks to the excellent corrosion resistance [5–8]. However, the low thermal conductivity of LTCC materials (around 3 to 5 W/m*k) limits their usage for power applications. Thermal vias are added to locally increase their thermal conductivity. Alternatively, a cut-out through the LTCC allows the bonding of the chip directly to the heat sink [9–11]. These designs lead to technological challenges like the CTE mismatch between the chip and the heat sink material. Thus, expensive heat sink materials with matched CTE, such as MoCu or WCu, are used. An alternative approach is to cool down the device with a coolant that is guided through fluidic channels inside the LTCC device [12–15].

In [16], the integration of a proprietary silver tape in LTCC for thermal management purposes is reported. The integration of silver tape in the LTCC provides paths with a high thermal conductivity. Hence, the thermal resistance of the critical path between power chip and heat sink can be reduced. In the presented investigation a commercially available silver tape is integrated in the LTCC during the co-fire process to form a through-substrate heat spreader. Fig. 1 shows a schematic cross-section of the silver head spreader.

The thermal performance of the heat spreader is investigated and compared with common thermal management solutions. Additionally, the interface between the LTCC and the silver structure is investigated for leaks, and the bond strength is measured.

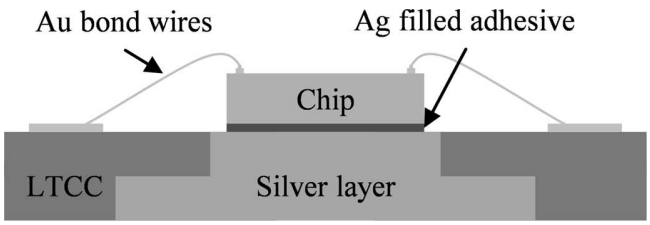

Fig. 1: Schematic cross-section through the silver heat spreader design, the chip is bonded directly to the silver structure.

II. Fabrication of the Silver Heat Spreader in LTCC DuPont 951 Green Tape™

The silver tape comprises organics filled with silver particles. A filling grade of more than 90 % is measured by means of energy-dispersive X-ray spectroscopy (EDX) analysis. The tape is sintered at temperatures higher than 600 °C in order to form a crystalline structure.

* Corresponding author: tilo.welker@tu-ilmenau.de

Fig. 2 shows an SEM image of the silver tape before and after sintering. A z-shrinkage of 35 % is measured with a horizontal pushrod dilatometer (NETZSCH DIL 402 E) when the tape is sintered in accordance with the recommended LTCC DuPont 951 sintering profile. The sheet thicknesses of the silver tape and the LTCC tape match at 254 µm so they can be easily combined. Openings and small plates are structured by means of laser-cutting (Q-switched Nd:YAG laser at a wavelength of 355 nm supplied by LPKF Laser & Electronics AG) into single LTCC tapes and the silver tape respectively. The heat spreader structure comprises two laser-cut LTCC sheets and two small silver plates (cf. Fig. 3). The stacked and aligned tapes are placed in a water-filled chamber, where they are laminated isostatically at a pressure of 210 bar and a temperature of 70 °C. The substrate is fired in a pressure-assisted constraint sintering process (1.7 kPa, 875 °C for 30 min).

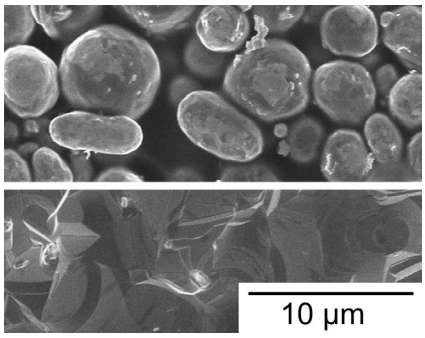

Fig. 2: SEM image of silver tape before (top) and after sintering (bottom). Unsintered material has a particle size distribution of 0.7 µm to 9 µm. Material sintered at 875 °C shows a crystalline structure.

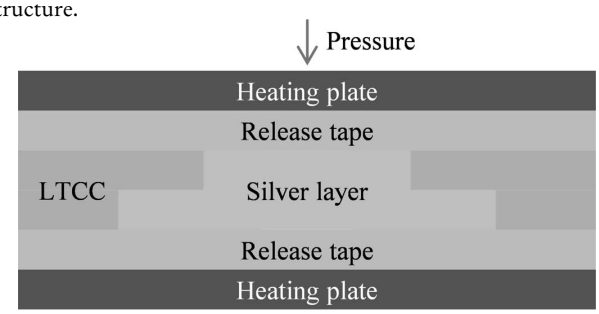

Fig. 3: Schematic cross-section through the sintering approach. Release tape is laminated to the stack to constrain the substrate during sintering.

The fired LTCC module has dimensions of 18 x 18 x 0.32 mm^3. The length of the silver heat spreader is 3 mm in the top layer and varies from 5 mm to 7 mm in the bottom layer. In Fig. 4, the cross-section through the right corner of the fabricated heat spreader is depicted. Slight pull-back of the silver structure from the surrounding LTCC can be observed.

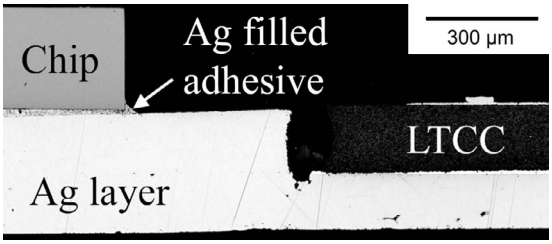

Fig. 4: Detailed cross-section through the right corner of the fabricated silver heat spreader. The chip is bonded with silver-loaded adhesive to the silver structure.

III. Experimental Procedure

(1) Evaluation of thermal performance

The thermal performance is evaluated based on measurement of the steady-state thermal resistance. A thermal test chip (PST1 – 02/5PU from Delphi) is bonded with silver-filled adhesive (λ = 60 W/mK) directly to the silver structure. The chip has an active area of 6.25 mm^2 and contains a planar resistor for resistive heating (P) and a temperature sensor (T_j). The module is placed on a temperature-controlled heat sink to get stable measuring conditions. The heat sink consists of a Peltier element, a water cooler and a copper heat spreader. The power of the Peltier element is regulated by a PID controller (TED4015, Thorlabs INC., stability ± 1 mK), which uses the heat spreader temperature as the present value. The heat spreader temperature (T_{GND}) is obtained from a thin-film RTD (Pt1000, ± 100 mK accuracy at 22 °C) which is integrated in the copper heat spreader 1 mm below the surface. Fig. 5 shows the schematic cross-section of the measurement arrangement.

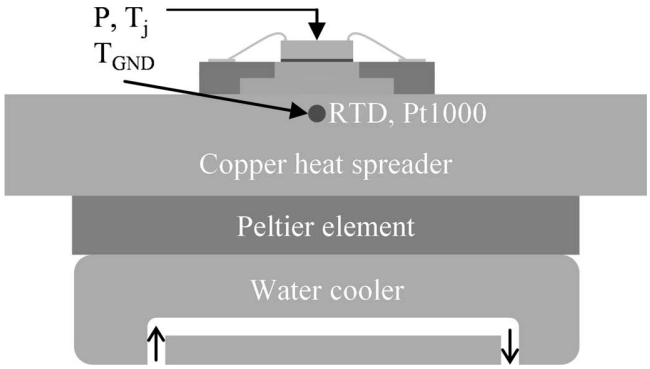

Fig. 5: Schematic cross-section through the measurement approach. The module with bonded thermal test chip is placed on a temperature-controlled heat sink.

A thermal load generated by resistive heating increases the junction temperature of the thermal test chip. At the point of thermal equilibrium the thermal resistance is calculated according to (1).

$$R_{th} = \frac{(T_j - T_{GND})}{P} \qquad (1)$$

The thermal resistances of three silver heat spreaders are measured. Three alternatives for thermal management are investigated utilizing the same approach and test chip, see Fig. 6. Hence, the cooling solutions can be easily compared. For this purpose a module with an array of 36 thermal vias made of silver paste (diameter: 250 µm, pitch: 500 µm) is fabricated and assembled with the thermal test chip. A second module allows the direct placement of the chip in a cavity. Here the test chip is bonded on a 1.5 mm-thick Mo30Cu heat spreader in a low-temperature silver sintering process.

The active cooling of the module with integrated fluidic channels is presented in previous works and compared to common thermal management solutions [15]. In this design, fluidic channels integrated in the LTCC guide a coolant through the module, which dissipates heat out of the module. The chip is placed on an array of 36 thermal vias which

transfer the heat into the fluidic channel. Water with a constant volume flow of 200 ml/min was used as coolant. The calculation of the thermal resistance was based on the temperature difference between the junction and fluidic inlet.

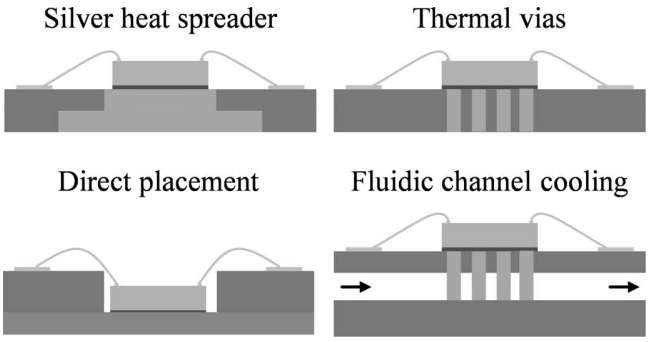

Fig. 6: Schematic cross-section through different cooling solutions.

(2) Testing for leaks

The leak tightness of the bond interface is tested in a helium leak test utilizing an evacuated chamber below the LTCC substrate [17]. For this purpose, the LTCC module is bonded with vacuum-tight glue on a vacuum adapter which is shown schematically in Fig. 7. The measurement arrangement is evacuated to 5 x 10^{-4} mbar through an opening in the adapter. A helium-enriched atmosphere is generated around the chamber at atmospheric pressure. A helium-sensitive mass spectrometer (SmartTest from Pfeifer Vacuum GmbH) detects any helium that flows through leaks in the bond interface into the chamber (cf. Fig. 7).

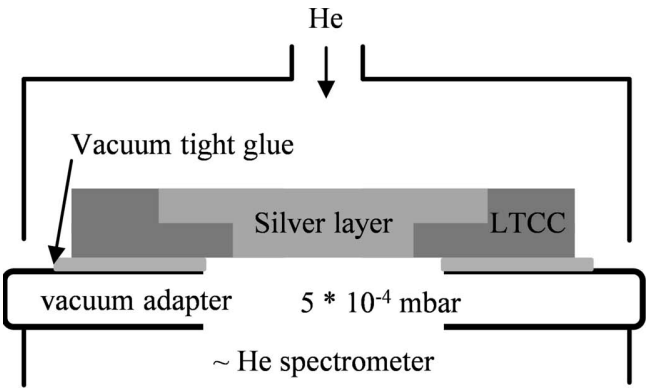

Fig. 7: Leak test with a He-sensitive mass spectrometer (vacuum method). The test sample is evacuated to 5 x 10^{-4} mbar and a helium-enriched atmosphere is generated around it.

(3) Measurement of the bond strength

The bonding strength is measured in a tension test. Therefore, silver plates (10 mm square) are buried into a LTCC substrate. Different silver layers (bonding agent A and B) are screen-printed on the LTCC layers in order to enhance the bond strength between the LTCC-silver plate interfaces. The substrate is cut in 10-mm-square pieces after firing. In the next step, retaining pins are glued to the bonded assembly. A tensile force is applied to the retaining pins by a tensile testing system (Z010 from Zwick GmbH & Co. KG) and the tensile force is measured. The testing approach allows tensile forces up to 2 kN (maximum tensile strength 8.8 N/mm^2 for the tested area). Fig. 8 shows the test approach.

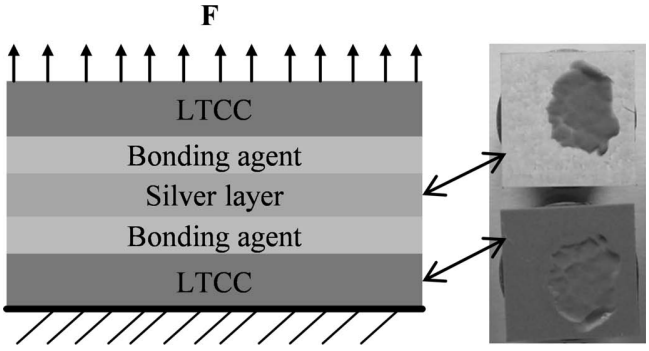

Fig. 8: Left: Schematic view of the approach for measuring the tensile strength; retaining pins are excluded. Right: Sample without bonding agent after test, the weak-point is the interface between the silver tape and the LTCC, cracks also occur in the LTCC.

IV. Results and Discussion

In Fig. 9 the thermal resistance of the tested cooling methods is compared. An exponential relationship between the length of the silver heat spreader and the thermal resistance is observed. It can be assumed that the heat spreading angle does not increase significantly when the spreading length is increased above a specific value. This length strongly depends on the chip length and the heat spreader thickness. Thus, the effective thermal resistance won't be affected above this point. The minimal thermal resistance is 1.2 K/W for the investigated chip with a length of 2.54 mm, which is nearly four times lower than the thermal resistance of the thermal via approach.

All fabricated bond interfaces show a leak rate over 5 x 10^{-5} mbar·l/s, which implies that the interface between the LTCC and the silver tape is not gas-tight. It is very likely that the slight pull-back of the silver structure from the surrounding LTCC generates voids in the bond interface, which are responsible for the leaks. Nevertheless, the bulk silver tape showed a leakage rate below 5 x 10^{-10} mbar·l/s when tested with the same approach. Therefore, it can be assumed that the silver material itself is densely sintered.

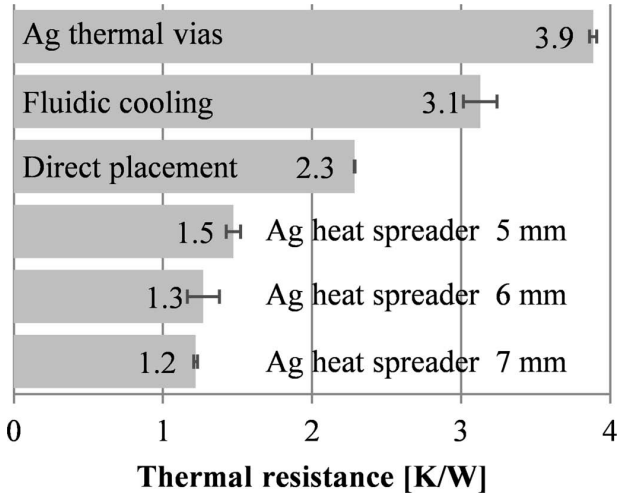

Fig. 9: Junction to case/junction to fluid resistance of common thermal management solutions in LTCC compared to the silver heat spreaders, ordered by size.

The measured tensile strengths of the bond interfaces are shown in Table 1. The bond interface between the LTCC and the silver plate failed before the test limit was achieved. Crack development in the LTCC could also be observed.

Table 1: Measured tensile strength of the LTCC-silver tape interface. The highest bonding strength is achieved with bonding agent A accompanied by a high deviation.

Bonding agent	Tensile strength [MPa]	Deviation [MPa]
Without	5.6	1.1
Ag Paste A	8.5	7.9
Ag Paste B	1.6	1.0

It is very likely that this is caused by induced thermal stress during the cooling step in the sintering process. This stress is caused by the CTE mismatch between the silver plate and the LTCC. The highest tensile strength is achieved with bonding agent A accompanied by a high deviation. The samples fabricated without a bonding agent show a slightly lower tensile strength with reduced deviation. Further investigations have to clarify the reason for the high deviation of the test samples with bonding agent A.

V. Conclusion

A thick silver heat spreader is integrated in a LTCC substrate during the co-firing process. The bonding strength evaluated in a tension test is 5.6 MPa for the samples without a bonding agent. The higher tensile strength of the samples with bonding agent A is accompanied by a high deviation. Hence, further work is required to ascertain the reason for the high deviation. The gas tightness of the bond interface could not be affirmed, but the silver tape seems to be densely sintered. The thermal resistance is measured with a thermal test chip and a temperature-controlled heat sink. With a thermal resistance of 1.2 K/W, the heat spreader is sufficient for many applications in the middle to lower power segment.

Acknowledgement

The presented work has been funded by Germany's Federal Ministry of Economic Affairs and Energy (funding code 50YB1303). The authors would like to thank their industrial partners for their support and T. Reimann and S. Bierlich (Jena University of Applied Sciences) for the shrinkage measurement during sintering.

References

1 Müller, J., Perrone, R., Drüe, K.-H., Stephan, R., Trabert, J.F., Hein, M.A., Schwanke, D., Pohlner, J., Reppe, G., Kulke, R., Uhlig, P., Jacob, A.F., Baras, T., Molke, A.: Comparison of high resolution patterning technologies for LTCC microwave circuits, *J. Microelectron. Electron. Packag.*, **4**, [3], 99 – 104, (2007).

2 Humbla, S., Kaleem, S., Müller, J., Rentsch, S., Stephan, R., Stöpel, D., Vogt, G., Hein, M.A.: On-orbit verification of a 4 × 4 switch matrix for space applications based on the low temperature Co-fired ceramics technology, *Frequenz*, 66, 11 – 12, (2012).

3 Schulz, A., Rentsch, S., Xia, L., Müller, R., Müller, J.: A low-loss fully embedded stripline parallel coupled BPF for applications using the 60 GHz band, *Int. J. Appl. Ceram. Technol.*, **10**, [2], 307 – 312, (2013).

4 Ariza, A.P.G., Müller, R., Wollenschläger, F., Schulz, A., Elkhouly, M., Sun, Y., Glisic, S., Trautwein, U., Stephan, R., Müller, J., Thomä, R.S., Hein, M.A.: 60 GHz ultrawideband polarimetric MIMO sensing for wireless multi-gigabit and radar, *IEEE T. Antenn. Propag.*, **61**, [4], 1631 – 1641, (2013).

5 Gross, G.A., Thelemann, T., Schneider, S., Boskovic, D., Köhler, J.M.: Fabrication and fluidic characterization of static micromixers made of low temperature cofired ceramic (LTCC), *Chem. Eng. Sci.*, **63**, [10], 2773 – 2784, (2008).

6 Bartsch de Torres, H., Rensch, C., Fischer, M., Schober, A., Hoffmann, M., Müller, J.: Thick film flow sensor for biological microsystems, *Sens. Actuat. A-Phys.*, **160**, [1 – 2], 109 – 115, (2010).

7 Geiling, T., Welker, T., Müller, J., Ehrling, C.: Design, Fabrication, and Operation of a Nitrogen Monoxide Measurement Device Based on LTCC, *J. Microelectron. Electron. Packag.*, **9**, [4], 171 – 177, (2012).

8 Welker, T., Geiling, T., Bartsch, H., Müller, J.: Design and fabrication of transparent and gas-tight optical windows in low-temperature co-fired ceramics, *Int. J. Appl. Ceram. Technol.*, **10**, [3], 405 – 412, (2013).

9 Zampino, M.A., Kandukuri, R., Jones, W.K.: High performance thermal vias in LTCC substrates. In: Proceedings of the 8th Intersociety Conference on Thermal and Thermomechanical Phenomena in Electronic Systems, San Diego, California, May 30 - June 1, 179 – 185, 2002.

10 Müller, J., Mach, M., Thust, H., Kluge, C., Schwanke, D.: Thermal design considerations for LTCC microwave packages. In: Proceedings of the 4th European Microelectronics and Packaging Symposium, Slovenia, Terme Čatež, May 21 – 24, 159 – 164, 2006.

11 Müller, J., Mach, M.: Thermal design considerations on wirebond packages. In: Proceedings of the 17th European Microelectronics and Packaging Conference and Exhibition, Rimini, Italy, June 15 – 18, 2009.

12 Thelemann, T., Thust, H., Bischoff, G., Kirchner, T.: Liquid cooled LTCC substrates for high power applications, *Int. J. Microcircuits Electron. Packag.*, **23**, [2], 209 – 214, (2000).

13 Adluru, H., Zampino, M.A., Liu, Y., Jones, K.W.: Embedded Heat Exchanger in LTCC Substrate. In: Proceedings of the IMAPS Conference and Exhibition on Ceramic Interconnect Technology, Denver, Colorado, April 7 – 9, 2003.

14 Barlow, F., Wood, J., Elshabini, A., Stephens, E.F., Feeler, R., Kemner, G., Junghans, J.: Fabrication of precise fluidic structures in LTCC, *Int. J. Technol. Appl. Ceram.*, **6**, [1], 18 – 23, (2009).

15 Welker, T., Müller, J.: Design and fabrication of integrated fluidic channels for liquid cooling of a LTCC device. In: Proceedings of the 10th International Conference and Exhibition on Ceramic Interconnect and Ceramic Microsystems Technologies, Osaka, Japan, April 14 – 16, 2014.

16 Wang, P., Jones, K.W., Liu, Y.: Thick silver tape in low temperature cofire ceramic (LTCC) for thermal management. In: Proceedings of the IMAPS 34th International Symposium on Microelectronics, Baltimore, Maryland, October 9 – 11, 384 – 388, 2001.

17 U.S. Department of Defense – Test Method Standard Microcircuits, MIL-STD-883, Rev. J, Method 1014.14 – Seal, 2014.